Secondary organic aerosol formation from semi- and intermediate-volatility organic compounds and glyoxal: Relevance of O/C as a tracer for aqueous multiphase chemistry

Eleanor M. Waxman, Katja Dzepina, Barbara Ervens, Julia Lee-Taylor, Bernard Aumont, Jose L. Jimenez, Sasha Madronich, Rainer Volkamer

Secondary organic aerosol formation from semi- and intermediate-volatility organic compounds and glyoxal: Relevance of O/C as a tracer for aqueous multiphase chemistry

Eleanor M. Waxman,[1,2] Katja Dzepina,[3] Barbara Ervens,[2,4] Julia Lee-Taylor,[5] Bernard Aumont,[6] Jose L. Jimenez,[1,2] Sasha Madronich,[5] and Rainer Volkamer[1,2]

Received 24 December 2012; revised 26 January 2013; accepted 27 January 2013; published 7 March 2013.

[1] The role of aqueous multiphase chemistry in the formation of secondary organic aerosol (SOA) remains difficult to quantify. We investigate it here by testing the rapid formation of moderate oxygen-to-carbon (O/C) SOA during a case study in Mexico City. A novel laboratory-based glyoxal-SOA mechanism is applied to the field data, and explains why less gas-phase glyoxal mass is observed than predicted. Furthermore, we compare an explicit gas-phase chemical mechanism for SOA formation from semi- and intermediate-volatility organic compounds (S/IVOCs) with empirical parameterizations of S/IVOC aging. The mechanism representing our current understanding of chemical kinetics of S/IVOC oxidation combined with traditional SOA sources and mixing of background SOA underestimates the observed O/C by a factor of two at noon. Inclusion of glyoxal-SOA with O/C of 1.5 brings O/C predictions within measurement uncertainty, suggesting that field observations can be reconciled on reasonable time scales using laboratory-based empirical relationships for aqueous chemistry. **Citation:** Waxman, E. M., K. Dzepina, B. Ervens, J. Lee-Taylor, B. Aumont, J.-L. Jimenez, S. Madronich, and R. Volkamer (2013), Secondary organic aerosol formation from semi- and intermediate-volatility organic compounds and glyoxal: Relevance of O/C as a tracer for aqueous multiphase chemistry, *Geophys. Res. Lett.*, *40*, 978–982, doi:10.1002/grl.50203.

1. Introduction

[2] Initially, models predicted secondary organic aerosol (SOA) formation from the gas-phase oxidation of specific precursor volatile organic compounds (VOCs) whose product saturation vapor pressures are low enough to partition to the aerosol phase [*Seinfeld and Pankow*, 2003]. This framework for SOA formation now includes semivolatile and intermediate volatility organic compounds (S/IVOCs) [*Robinson et al*., 2007; *Grieshop et al*., 2009]. Inclusion of S/IVOCs significantly improved predictions of SOA mass in polluted areas [*Dzepina et al*., 2009, 2011; *Hodzic et al*., 2010; *Lee-Taylor et al*., 2011], but reveals shortcomings in predicting chemical properties such as the atomic oxygen-to-carbon ratio (O/C ratio) on short aging time scales [*Dzepina et al*., 2009].

[3] During the Mexico City Metropolitan Area (MCMA-2003) case study on 9 April 2003, rapid SOA formation produced significantly more aerosol mass than expected [*Volkamer et al*., 2006], which was mostly attributed to the rapid aging of S/IVOCs [*Dzepina et al*., 2009]. Simultaneously, less gas-phase glyoxal was observed than predicted by a gas-phase mechanism that did not consider particle-phase partitioning or processing [*Volkamer et al*., 2007]. It was hypothesized that this imbalance could be due to SOA formation from glyoxal because it is highly soluble and quite reactive in the aqueous phase. Glyoxal is likely to add to SOA through multiphase reactions where it can contribute a small amount of mass with a very high O/C ratio due to its ability to form low-volatility, high molecular weight products in the aerosol aqueous phase [e.g. *Volkamer et al*., 2009; *Hennigan et al*., 2009; *Lim et al*., 2010; *Ervens et al*., 2011].

[4] Oxygen-to-carbon ratios are primarily used as a metric for relating organic aerosol (OA) chemical composition to aerosol age, hygroscopicity, and volatility [*Ng et al*., 2007; *Jimenez et al*., 2009]. However, they can also provide a means to test our process level understanding of SOA formation mechanisms. During this case study the observed O/C from oxygenated organic aerosol (OOA) was significantly higher than predicted [*Dzepina et al*., 2009]. This imbalance is currently not understood, and no previous attempts have been made to understand O/C based on a molecular modeling perspective of SOA. Here we compare the O/C time evolution as measured by aerosol mass spectrometry (AMS) to results from a molecular modeling perspective to test our mechanistic understanding of SOA formation, including—for the first time—treatment of both S/IVOC gas-phase and aerosol multiphase chemical reactions.

2. Description of Model Approaches

2.1. Chemical Mechanism of Glyoxal Reactions in Aerosol Water

[5] To predict the amount of SOA formed from glyoxal, we apply an observationally-constrained box model that simulates

All supporting information may be found in the online version of this article.

[1]Department of Chemistry and Biochemistry, University of Colorado Boulder, 215 UCB, Boulder, Colorado, 80309, USA.
[2]CIRES, University of Colorado Boulder, 216 UCB, Boulder, Colorado, 80309, USA.
[3]Department of Chemistry, Michigan Technological University, 1400 Townsend Dr., Houghton, Michigan, 49931, USA.
[4]Chemical Sciences Division, NOAA/ESRL, 325 Broadway, Boulder, Colorado, 80305, USA.
[5]National Center for Atmospheric Research, P.O. Box 3000, Boulder, Colorado, 80307, USA.
[6]LISA, UMR CNRS/INSU 7583, Université Paris Est Créteil et Université Paris Diderot, Créteil, France.

Corresponding author: R. Volkamer, University of Colorado Boulder, Department of Chemistry, 215 UCB, Boulder, CO 80309 USA. (rainer.volkamer@colorado.edu)

0094-8276/13/10.1002/grl.50203

processing of glyoxal in aerosol water based on a laboratory-derived glyoxal-SOA (GLY-SOA) mechanism [*Ervens and Volkamer*, 2010]. We constrain the model with ambient measurements from 9 April 2003 in Mexico City to determine if glyoxal uptake and aqueous-phase processing can explain the glyoxal imbalance from MCMA-2003.

[6] Secondary organic aerosol formation is represented in the model as a surface-limited uptake process, bulk-phase reactions, or a combination of the two [see *Ervens and Volkamer*, 2010, Figure 1]. Briefly, the mechanism includes partitioning of glyoxal into aerosol water based on its Henry's law constant and explicit hydration reactions to form the monohydrate and dihydrate using the kinetic and equilibrium constants derived by *Ervens and Volkamer* [2010]. This results in a very high effective Henry's law value of 4.2×10^5 M/atm [*Ip et al.*, 2009]. These species then become part of an organic aqueous phase where they undergo further processing, including oligomerization and reactions with OH and ammonium. Sensitivity studies were carried out that varied the mass accommodation coefficient α (physical uptake parameter), reactive uptake coefficient γ (includes aqueous phase reactivity), OH-radical concentration, Henry's law constant for unhydrated glyoxal (H), and SOA hygroscopicity κ. The model parameters, ambient observations used as model constraints, and predicted GLY-SOA mass from individual simulations are shown in Table S1 and further model details are included in the Supporting Information.

2.2. Chemical Mechanisms of S/IVOC Aging

[7] The representation of gas-phase S/IVOC aging to date is largely based on empirical parameterizations, except for the few mechanisms that utilize explicit chemistry such as GECKO-A (Generator of Explicit Chemistry and Kinetics of Organics in the Atmosphere) [*Aumont et al.*, 2005; *Camredon et al.*, 2007] or the near-explicit Leeds Master Chemical Mechanism [*Bloss et al.*, 2005]. Empirical representations such as the volatility basis set (VBS) prescribe oxygen addition and volatility decreases for each gas phase oxidation step. Two prominent VBS approaches to S/IVOC aging, *Robinson et al.* [2007] (ROB) and *Grieshop et al.* [2009] (GRI), are treated as described above and used here as done in *Dzepina et al.* [2009]. The major differences between these two approaches are that ROB uses an OH rate constant of 4.0×10^{-11} cm^3 molec^{-1} s^{-1}, an oxygen addition of 1.075 per generation, and the volatility of a compound is shifted by one bin, while GRI uses an OH rate constant of 2.0×10^{-11} cm^3 molec^{-1} s^{-1}, an oxygen addition of 1.4 per generation, and compounds are shifted by two volatility bins [*Robinson et al.*, 2007; *Grieshop et al.*, 2009].

[8] We compare these parameterizations with a third mechanism, GECKO-A, which uses an explicit molecular-based approach to S/IVOC oxidation and gas-particle partitioning. GECKO-A self-generates chemical mechanisms via structure-activity relationships based on our current understanding of gas-phase chemistry and kinetics. S/IVOCs are oxidized by OH, O_3, and NO_3; peroxy radical intermediates react with NO, NO_2, NO_3, HO_2, or RO_2, and alkoxy radicals react with O_2 and undergo isomerization and decomposition reactions [*Aumont et al.*, 2005; *Camredon et al.*, 2007]. As in *Lee-Taylor et al.* [2011], the mechanism presented here uses *n*-alkanes to represent all S/IVOC precursors.

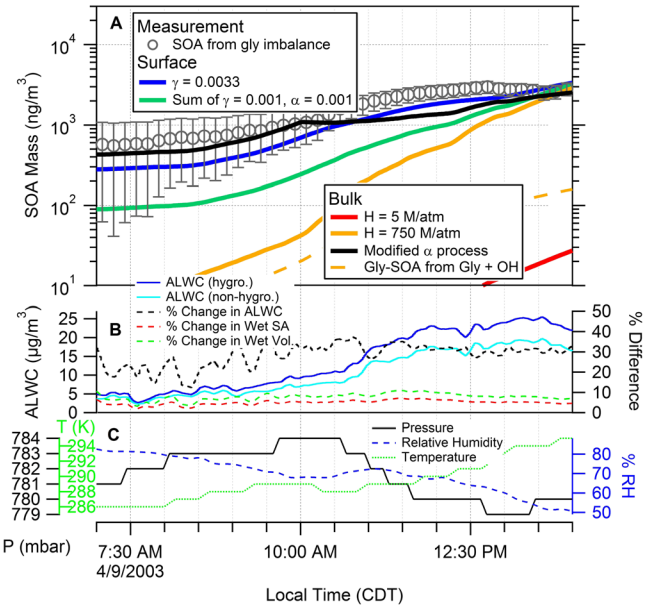

Figure 1. Comparison of temporal evolution of GLY-SOA as predicted by the model with that calculated from the measured glyoxal imbalance. (A) GLY-SOA mass shown for five cases: bulk processes using H for dilute aqueous phase (red) and aerosol water (orange), surface processes using Mexico City-derived uptake coefficients (γ) (blue), results from a bulk process using time-resolved α and γ (black, see Supporting Information), and results from including a surface process with no bulk reactions and a bulk reaction with no surface process (green). Grey circles denote the glyoxal imbalance from *Volkamer et al.* [2007]. (B) Difference (%) between Aerosol Liquid Water Content (ALWC, black), wet aerosol surface area (red), and wet aerosol volume (green) between the hygroscopic and non-hygroscopic SOA cases. (C) Input data for temperature, pressure, and RH.

2.3. Calculation of the O/C Ratio of the Organic Aerosol Fraction

[9] All O/C ratios discussed herein are atomic, and all simulations begin at midnight Central Daylight Time (local time). We use four components to calculate the total SOA O/C ratios: (1) background SOA (BG-SOA), OOA measured before sunrise which is either present at night or results from mixing in from the residual layer aloft in the morning [*Dzepina et al.*, 2009]; (2) VOC SOA (V-SOA), predicted from gas-phase precursor measurements of, e.g., single-ring aromatics, as described by *Dzepina et al.* [2009]; (3) S/IVOC-SOA (SI-SOA) predicted from VBS parameterizations of emissions of $C_{\geq 11}$ according to the oxidation parameterizations of ROB or GRI, or the GECKO-A oxidation mechanism; and (4) glyoxal SOA (GLY-SOA), as described in section 2.1. The O/C ratios for V-SOA and the ROB and GRI SI-SOA are taken from the literature and previous model results [*Robinson et al.*, 2007; *Grieshop et al.*, 2009; *Dzepina et al.*, 2009]. The O/C ratios for GECKO-A SI-SOA and GLY-SOA are calculated in situ, and the O/C for BG-SOA was measured in Mexico City (see Supporting Information). We perform a second O/C comparison for total OA that also includes hydrocarbon-like organic aerosol (HOA) measured by the AMS, or primary organic aerosol (POA) calculated from GECKO-A. This second analysis

thus avoids the possibility of bias from comparing the SOA surrogate "OOA" to SOA predictions by models.

3. Model Results and Discussion

3.1. Modeled GLY-SOA Formation in Mexico City

[10] The difference between the gas-phase glyoxal predicted to be formed in Mexico City and the amount actually measured is termed the glyoxal imbalance, which was hypothesized to be due to particle uptake [*Volkamer et al*., 2007]. The amount of GLY-SOA predicted by our laboratory-based mechanism can explain our previous estimate of the imbalance on similar time scales to those measured in Mexico City (Figure 1). The temporal evolution of the predicted GLY-SOA shows a very different time trace depending on whether a bulk process or a surface process is represented in the box model. Calculations using a surface-limited process match the shape of the imbalance better than calculations using bulk phase reactions, with best agreement for $\gamma = 0.0033$. The rate of glyoxal uptake to aerosols is generally compatible with laboratory-measured γ values. The optimum γ of 0.0033 is slightly lower than the γ of 0.0037 derived in *Volkamer et al*. [2007] to account for the previously neglected water uptake by the organic fraction of the aerosols. Similar γ values have been observed in chamber experiments; *Liggio et al*. [2005] and *Trainic et al*. [2011] show comparable aerosol mass growth rates. The kinetics of glyoxal mass transfer can vary by several orders of magnitude between laboratory experiments [*Kroll et al*., 2005; *Galloway et al*., 2011; *Nakao et al*., 2012]; the reasons for this variability are as of yet unclear. In our case study, about 1 in every 300 collisions of glyoxal with surfaces of the metastable particles on average results in uptake.

[11] The product distribution from glyoxal reactions in the bulk aerosol changes as a function of time of day (see Table S1). Reactions with ammonium increase in relative importance over OH radical reactions in the later morning, due to increasing NH_4^+ aerosol mass (see Figure S1A). The product distribution is most sensitive to the H value for glyoxal and particle pH, and it only weakly depends on gas-phase OH radical concentrations. The SOA mass formed from OH radical reactions with glyoxal in the aqueous phase is added as a dashed orange line in Figure 1 and accounts at maximum for 5.5% of the GLY-SOA. Gas-phase OH is the only OH source considered in particles during these model runs (Figure S2). Additional radical sources are not considered, but may result from organic photochemistry in aerosol water [*Volkamer et al*., 2009; *Monge et al*., 2012]. With increasing H and pH, the ammonium reaction gains in relative importance because the NH_4^+ availability is not mass transfer limited; at lower H the OH-radical reaction is relatively more important. The rate constant of glyoxal with NH_4^+ is a strong function of pH [*Noziere et al*., 2009], which is constant ($pH \sim 4$) during this case study based on thermodynamic modeling using ISORROPIA [*Volkamer et al*., 2007] constrained by aerosol composition and gas-phase ammonia measurements. The aerosol composition on 9 April [*Salcedo et al*., 2006] compares closely to other days, when the pH is slightly higher [*San Martini et al*., 2006]. Reaction channels other than NH_4^+ gain in relative importance at lower pH, where the overall rate of GLY-SOA formation is lower than at high pH. Our results apply to the conditions in Mexico City, and a similar analysis in other urban environments will need to characterize parameters including H, pH, LWC, and aerosol phase state, which all influence the rate of GLY-SOA formation.

3.2. Comparison of Model SOA O/C and Mass with Measurements

[12] The SOA formed from S/IVOC oxidation is predicted to dominate overall SOA mass. Comparable SI-SOA amounts are predicted from ROB and GECKO-A simulations (Figure 2). GRI results in the highest SI-SOA mass and O/C predictions, consistent with previous work [*Dzepina et al*., 2011]. The sum of HOA measured by AMS (or POA predicted by the GECKO-A model), BG-SOA, V-SOA, GLY-SOA, and either ROB or GECKO-A is very close to the OA mass measured by the AMS, while using GRI as the SI-SOA component significantly over-estimates OA mass (Figure 2b).

[13] Figure 2a compares the O/C ratio of the individual OA components. For an integral OH exposure over the time period of 7 A.M. to 2 P.M. (up to 4.5×10^6 molecules/cm^3 as shown in Figure S3-F) and defined as $\int[OH]dt$, of 1.8×10^{10} molec cm^{-3}·s (4.7×10^{10} molec cm^{-3}·s) at 11 am (2 pm), the O/C ratios are 0.5 (0.6), 0.11 (0.16) and 0.12 (0.13) for the GRI, ROB and GECKO-A SOA components, respectively. GECKO-A shows the slowest rate of O/C increase among these three aging mechanisms: at 9 A.M., the O/C is 0.12 and O/C has increased by 10% at 2 P.M. In contrast, the O/C predicted from ROB doubles from 0.082 at 7 A.M. to 0.16 by 2 P.M., and the GRI O/C is 0.43 at 7 A.M., and increases by 40% by 2 P.M. The slow rate of O/C increase from GECKO-A SI-SOA extends to longer aging time scales as well ($O/C_{SOA,C16} < 0.25$ at $\int[OH]dt = 1.7 \times 10^{11}$ molec cm^{-3} s) [*Aumont et al*., 2012], generally consistent with laboratory observations [*Lambe et al*., 2012].

[14] Predicted OA O/C is compared to observations in Figure 2c. For the solid lines, four components (BG-SOA, V-SOA, SI-SOA, and POA) are used to calculate O/C for three cases that differ only in the SI-SOA parameterization: Case 1 (ROB), Case 2 (GRI), and Case 3 (GECKO-A). In the absence of GLY-SOA, Case 2 overestimates both SOA mass and O/C, and this VBS parameterization is therefore deemed unrealistic. Cases 1 and 3 underestimate the AMS-measured O/C ratio. The dashed lines in Figure 2c show the predicted O/C when the contribution of GLY-SOA (section 2.1) is included, using a GLY-SOA O/C of 1.5, which was selected as close to the middle of the range of O/C values of 1 to 1.8 observed in laboratory studies [*Lim et al*., 2010; *Chhabra et al*., 2010; *Lee et al*., 2011]. With the addition of GLY-SOA better agreement is observed between Cases 1 and 3 and the AMS data. Sensitivity studies indicate that the total SOA O/C is rather insensitive to BG-SOA in the afternoon. BG-SOA transport thus cannot explain the O/C mismatch, discussed further in the Supporting Information. A similar analysis was done comparing total SOA only, and shows similar results (see Figure S6 and Supporting Information).

[15] Accurate predictions of aerosol O/C are important for estimating the magnitude of climate change. O/C shows a strong linear correlation with aerosol hygroscopicity [*Jimenez et al*., 2009; *Chang et al*., 2010]. As O/C increases, the aerosol becomes more hygroscopic, and thus larger due to water absorption. This results in a lower

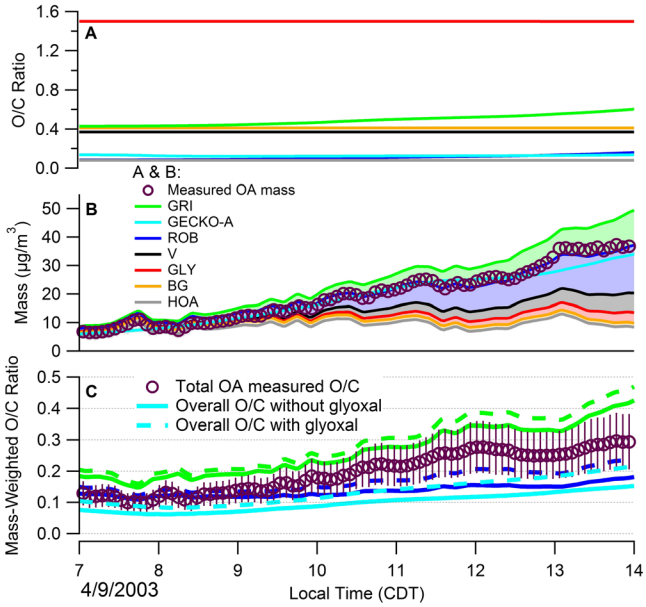

Figure 2. Comparison of measured and predicted O/C for different mechanisms. (A) Time-dependent O/C ratios for each OA component. (B) Temporal evolution of predicted OA mass for each component. The sum of HOA + BG-SOA + V-SOA + GLY-SOA + ROB SI-SOA or GECKO-A SOA matches the value of the measured OA mass, but GRI SI-SOA overestimates. (C) Comparison between O/C ratios measured in Mexico City and predicted by the mechanisms as described in section 2.3. Green lines: includes GRI SI-SOA; blue lines: includes ROB SI-SOA; turquoise lines: includes GECKO-A SOA from $C_{\geq 11}$ species. Solid lines: BG-SOA + V-SOA + SI-SOA but no GLY-SOA. Dashed lines: include GLY-SOA with an O/C of 1.5.

critical supersaturation at which the aerosol can behave as a cloud condensation nuclei [*Petters and Kreidenweis*, 2007]. There is additional evidence that the aerosol O/C is correlated with aerosol scattering cross-sections [*Cappa et al.*, 2011]. Thus, accurately modeling aerosol O/C is important not only to test our understanding of SOA formation mechanisms, but also for predictions of the aerosol direct effect (scattering incident radiation) and the aerosol indirect effect (cloud formation).

4. Conclusions and Outlook

[16] For the first time, the glyoxal imbalance from *Volkamer et al.* [2007] was evaluated using a laboratory-based model. A surface-limited process is found to best reproduce the time evolution of the glyoxal imbalance with an uptake coefficient, $\gamma = 0.0033$, consistent with laboratory data [*Liggio et al.*, 2005; *Trainic et al.*, 2011]. For the bulk reaction case, the GLY-SOA product distribution depends strongly on the Henry's law constant of glyoxal and particle pH, and less on the gas-phase OH radical concentration. When the only source for aqueous phase OH radicals is transfer from the gas-phase, the SOA mass formed from aqueous phase OH radical reactions is very small (≤5% of GLY-SOA); additional radical sources from organic photochemistry are likely [*Volkamer et al.*, 2009; *Monge et al.*, 2012]. The dominant GLY-SOA formation route in the model is from the catalytic reaction with NH_4^+ at the elevated particle pH in Mexico City (Table S1).

[17] Although S/IVOCs are predicted to contribute most (50–70%) of the SOA mass, the comparison of different S/IVOC aging schemes gives little confidence in predicting the observed O/C ratio over aging times equivalent to 4.7×10^{10} molec cm^{-3} s OH exposure (~ 4.3 h at [OH] = 3×10^6 molec cm^{-3}). The GECKO-A model was found to produce SI-SOA with substantial mass yields, but mostly in a reduced state (O/C < 0.13) that does not match the highly oxygenated OA component typically found in situ. The sum of SI-SOA, V-SOA, and BG-SOA can account for only about half the observed O/C during the afternoon. These results suggest a gap in our understanding of the gas phase oxidation and/or efficient chemistry occurring in the condensed phase. We conclude that aqueous phase processing helps to explain the observed time evolution of aerosol O/C on rapid time scales similar to those observed in Mexico City. While GLY-SOA alone can only explain 30–50% of the O/C gap, glyoxal serves as an indicator for other soluble molecules that may undergo multiphase chemistry (e.g. methyl glyoxal, glycolaldehyde). More laboratory work is needed to identify reaction products from glyoxal and other soluble molecules that undergo aqueous multiphase chemistry, in particular to constrain their gas/aqueous phase partitioning, pH, ALWC, and aerosol phase state dependence of the rate of SOA formation.

[18] **Acknowledgments**. E.M.W. is the recipient of an NSF graduate fellowship. R.V. acknowledges financial support from US National Science Foundation CAREER award (ATM-0847793), and US Department of Energy, Office of Science award DE-SC0006080. B.E. acknowledges support from NOAA's Climate Goal. J.L.T. and S.M. were supported in part by grant DE-FG02-ER65323 from the US Department of Energy Office of Science. The National Center for Atmospheric Research is sponsored by the National Science Foundation. B.A. acknowledges support from the primequal program of the French Ministry of Ecology, Sustainable Development and Energy. We thank P. Ziemann for insightful discussions.

References

Aumont, B., S. Szopa, and S. Madronich (2005), Modelling the evolution of organic carbon during its gas-phase tropospheric oxidation: development of an explicit model based on a self generating approach, *Atmos. Chem. Phys.*, *5*, 2497–2517.

Aumont, B., et al. (2012), Modeling SOA formation from the oxidation of intermediate volatility *n*-alkanes, *Atmos. Chem. Phys.*, *12*, 7577–7589.

Bloss, C., et al. (2005), Development of a detailed chemical mechanism (MCMv3.1) for the atmospheric oxidation of aromatic hydrocarbons, *Atmos. Chem. Phys.*, *5*, 641–664.

Camredon, M., et al. (2007), The SOA/VOC/NOx system: an explicit model of secondary organic aerosol formation, *Atmos. Chem. Phys.*, *7*, 5599–5610.

Cappa, C. D., D. L. Che, S. H. Kessler, J. H. Kroll, and K. R. Wilson (2011), Variations in organic aerosol optical and hygroscopic properties upon heterogeneous OH oxidation, *Geophys. Res. Lett.*, *116*, D15204.

Chang, R. Y., et al. (2010), The hygroscopicity parameter (K) of ambient organic aerosol at a field site subject to biogenic and anthropogenic influences: relationship to degree of aerosol oxidation, *Atmos. Chem. Phys.*, *10*, 5047–5064.

Chhabra, P. S., R. C. Flagan, and J. H. Seinfeld (2010), Elemental analysis of chamber organic aerosol using an aerodyne high-resolution aerosol mass spectrometer, *Atmos. Chem. Phys.*, *10*, 4111–4131.

Dzepina, K., et al. (2009), Evaluation of recently-proposed secondary organic aerosol models for a case study in Mexico City, *Atmos. Chem. Phys.*, *9*, 5681–5709.

Dzepina, K., et al. (2011), Modeling the multiday evolution and aging of secondary organic aerosol during MILAGRO 2006, *Environ. Sci. Technol.*, *45*, 3496–3503.

Ervens, B., B. J. Turpin, and R. J. Weber (2011), Secondary organic aerosol formation in cloud droplets and aqueous particles (aqSOA): a

review of laboratory, field and model studies, *Atmos. Chem. Phys.*, *11*, 11069–11102.

Ervens, B., and R. Volkamer (2010), Glyoxal processing by aerosol multiphase chemistry: towards a kinetic modeling framework of secondary organic aerosol formation in aqueous particles, *Atmos. Chem. Phys.*, *10*, 8219–8244.

Galloway, M. M., C. L. Loza, P. S. Chhabra, A. W. H. Chan, L. D. Yee, J. H. Seinfeld, and F. N. Keutsch (2011), Analysis of photochemical and dark glyoxal uptake: Implications for SOA formation, *Geophys. Res. Lett.*, *38*, L17811.

Grieshop, A. P., et al. (2009), Laboratory investigation of photochemical oxidation of organic aerosol from wood fires 1: measurement and simulation of organic aerosol evolution, *Atmos. Chem. Phys.*, *9*, 1263–1277.

Hennigan, C. J., et al. (2009), Gas/particle partitioning of water-soluble organic aerosol in Atlanta, *Atmos. Chem. Phys.*, *9*, 3613–3628.

Hodzic, A., et al. (2010), Modeling organic aerosols in a megacity: potential contribution of semi-volatile and intermediate volatility primary organic compounds to secondary organic aerosol formation, *Atmos. Chem. Phys.*, *10*, 5491–5514.

Ip, H. S. S., X. H. H. Huang, and J. Z. Yu (2009), Effective Henry's law constants of glyoxal, glyoxylic acid, and glycolic acid, *Geophys. Res. Lett.*, *36*, L01802.

Jimenez, J. L., et al. (2009), Evolution of organic aerosols in the atmosphere, *Science*, *326*, 1525–1529.

Kroll, J., N. Ng, S. Murphy, R. Flagan, and J. Seinfeld (2005), Secondary organic aerosol formation from isoprene photooxidation under high-NO (x) conditions, *Geophys. Res. Lett.*, *32*, L18808.

Lambe, A. T., et al. (2012), Transitions from functionalization to fragmentation reactions of laboratory secondary organic aerosol (SOA) generated from the OH oxidation of alkane precursors, *Environ. Sci. Technol.*, *15*, 5430–5437.

Lee, A. K. Y., et al. (2011), Aqueous-Phase OH oxidation of glyoxal: Application of a novel analytical approach employing aerosol mass spectrometry and complementary off-line techniques, *J. Phys. Chem. A*, *115*, 10517–10526.

Lee-Taylor, J., et al. (2011), Explicit modeling of organic chemistry and secondary organic aerosol partitioning for Mexico City and its outflow plume, *Atmos. Chem. Phys.*, *11*, 13219–13241.

Liggio, J., S. Li, and R. McLaren (2005), Reactive uptake of glyoxal by particulate matter, *J. Geophys. Res. Atmos.*, *110*, D10304.

Lim, Y. B., et al. (2010), Aqueous chemistry and its role in secondary organic aerosol (SOA) formation, *Atmos. Chem. Phys.*, *10*, 10521–10539.

Monge, M. E., et al. (2012), Alternative pathway for atmospheric particles growth, *Proc. Nat. Acad. Sci.*, *109*, 6840–6844.

Nakao, S., et al. (2012), Chamber studies of SOA formation from aromatic hydrocarbons: observation of limited glyoxal uptake, *Atmos. Chem. Phys.*, *12*, 3927–3937.

Ng, N. L., et al. (2007), Secondary organic aerosol formation from m-xylene, toluene, and benzene, *Atmos. Chem. Phys.*, *7*, 3909–3922.

Noziere, B., P. Dziedzic, and A. Cordova (2009), Products and kinetics of the liquid-phase reaction of glyoxal catalyzed by ammonium ions (NH_4^+), *J. Phys. Chem. A*, *113*, 231–237.

Petters, M. D., and S. M. Kreidenweis (2007), A single parameter representation of hygroscopic growth and cloud condensation nucleus activity, *Atmos. Chem. Phys.*, *7*, 1961–1971.

Robinson, A. L., et al. (2007), Rethinking organic aerosols: Semivolatile emissions and photochemical aging, *Science*, *315*, 1259–1262.

Salcedo, D., et al. (2006), Characterization of ambient aerosols in Mexico City during the MCMA-2003 campaign with Aerosol Mass Spectrometry: Results from the CENICA Supersite, *Atmos. Chem. Phys.*, *6*, 925–946.

San Martini, F. M., et al. (2006), Implementation of a Markov Chain Monte Carlo Method to inorganic aerosol modeling of observations from the MCMA-2003 Campaign. Part II: Model application to the CENICA, Pedregal and Santa Ana sites, *Atmos. Chem. Phys.*, *6*, 4889–4904.

Seinfeld, J., and J. Pankow (2003), Organic atmospheric particulate material, *Annu. Rev. Phys. Chem.*, *54*, 121–140.

Trainic, M., et al. (2011), The optical, physical and chemical properties of the products of glyoxal uptake on ammonium sulfate seed aerosols, *Atmos. Chem. Phys.*, *11*, 9697–9707.

Volkamer, R. M., P. J. Ziemann, and M. J. Molina (2009), Secondary organic aerosol formation from acetylene (C_2H_2): Seed effect on SOA yields due to organic photochemistry in the aerosol aqueous phase, *Atmos. Chem. Phys.*, *9*, 1907–1928.

Volkamer, R. M., F. S. Martini, L. T. Molina, D. Salcedo, J. L. Jimenez, and M. J. Molina (2007), A missing sink for gas-phase glyoxal in Mexico City: Formation of secondary organic aerosol, *Geophys. Res. Lett.*, *34*, L19807.

Volkamer, R., J. L. Jimenez, F. San Martini, K. Dzepina, Q. Zhang, D. Salcedo, L. T. Molina, D. R. Worsnop, and M. J. Molina (2006), Secondary organic aerosol formation from anthropogenic air pollution: Rapid and higher than expected, *Geophys. Res. Lett.*, *33*, L17811.